Opto-Electronics Review 29 (2021) 80-84

PAN POLISH ACADEMY OF SCIENCES

Opto-Electronics Review

journal homepage: http://journals.pan.pl/opelre

Numerical analysis of the compositional graded quaternary barrier AlGaN-based ultraviolet-C light-emitting diode

S. Malik [a], M. Usman [a*], M. Hussain [b], M. Munsif [a], S. Khan [a], S. Rasheed [a], S. Ali [a]

[a] Faculty of Engineering Sciences, Ghulam Ishaq Khan Institute of Engineering Sciences and Technology, Topi, 23460, Khyber Pakhtunkhwa, Pakistan
[b] Faculty of Computer Sciences and Engineering, Ghulam Ishaq Khan Institute of Engineering Sciences and Technology, Topi, 23460, Khyber Pakhtunkhwa, Pakistan

Article info

Article history:
Received 14 Apr. 2021
Received in revised form 12 Jul. 2021
Accepted 19 Jul. 2021

Keywords:
ultraviolet, light-emitting diodes, efficiency, quantum wells

Abstract

The compositional graded quaternary barriers (GQBs) instead of ternary/conventional quantum barriers (QBs) have been used to numerically enhance the efficiency of AlGaN-based ultraviolet light-emitting diode (LED). The performance of LED with GQBs is examined through carrier concentrations, energy band diagrams, radiative recombination, electron and hole flux, internal quantum efficiency (IQE), and emission spectrum. As a function of the operating current density, a considerable reduction in efficiency droop is observed in the device with composition-graded quaternary barriers as compared to the conventional structure. The efficiency droop in case of a conventional LED is ~77% which decreased to ~33% in case of the proposed structure. Moreover, the concentration of electrons and holes across the active region in case of the proposed structure is increased to ~156% and ~44%, respectively.

1. Introduction

Considerable attention has been directed towards the improvement of $Al_xGa_{1-x}N$-based deep ultraviolet light-emitting diodes (DUV LEDs) due to their extensive range of promising applications, i.e., water and air purification, medical phototherapy, ultraviolet (UV) curing, and surface disinfection, etc. UV radiation, between 260–280 nm, is more useful for the sterilization and purification process [1-4]. Moreover, DUV LEDs have extensive applications in suppressing different viruses present at different places like hospitals, care centres, as well as in quarantine centres [5,6]. DUV has also been reported to counteract the effects of the coronavirus (SARS-CoV-2) severe acute respiratory syndrome, which is the cause of the novel coronavirus disease 2019 (COVID-19) [7]. More importantly, AlGaN has attained a considerable attention due to its direct energy band gap transition between 3.4 and 6.2 eV [8,9]. However, UV LEDs still have comparatively low efficiency and emission power compared to $In_xGa_{1-x}N$-based visible LEDs [9-12]. Reasons behind the lower efficiency of UV LEDs mainly include the presence of high dislocation density [13] and p-doping issues in $Al_xGa_{1-x}N$. To overcome these issues, various solutions have been suggested by scientists such as multiquantum barrier electron blocking layers to enhance the device efficiency [14] and n-doped barrier to enhance the optoelectronic characteristics [15]. Moreover, to reduce the polarization between barrier layers and the well, a high Al-content AlGaN layer has been employed in quantum walls (QWs) [16]. Band-engineered QWs have also been employed to enhance the device efficiency [17-20]. In addition, engineered electron blocking layers (EBLs) have also been used to improve the device performance [20-25] among few other designs [26,27].

In this study, conventional quantum barriers (QBs) AlGaN were replaced by compositional graded quaternary barriers (GQBs) AlInGaN and their effects on the performance of DUV LEDs were numerically analysed. Researchers have employed AlInGaN in QWs for the UV emission [28]. In addition, AlInGaN superlattice has been used in EBLs [29] and graded AlInGaN barriers have also been demonstrated [30]. AlInGaN has been successfully grown with the pulse atomic layer epitaxy [31], as well as

*Corresponding author at: m.usman@giki.edu.pk

https://doi.org/10.24425/opelre.2021.135831
1896-3757/ Association of Polish Electrical Engineers (SEP) and Polish Academic of Sciences (PAS). Published by PAS

the pulsed metalorganic chemical vapor deposition (MOCVD) technique [32].

2. Methodology

Two different AlGaN-based LEDs have been theoretically studied by using the state-of-the-art simulation tool, i.e., SiLENSe 5.14. LED-A consists of five $Al_{0.45}Ga_{0.55}N$ QWs, each QW has a thickness of 2 nm. Each QW is placed between two $Al_{0.55}Ga_{0.45}N$ QBs, the thickness of each QB is of 10 nm. n-AlGaN and p-GaN layers are used for the injection of charge carriers into the QWs. The thickness and doping concentration in an n-AlGaN layer is of 300 nm and 5×10^{18} cm^{-3}, respectively while in a p-GaN layer a thickness is of 100 nm and a doping concentration is of 1×10^{20} cm^{-3}, respectively. Moreover, a p-$Al_{0.65}Ga_{0.35}N$ EBL with a thickness of 15 nm and a p doping of 5×10^{19} cm^{-3} is used. LED-B is similar to LED-A except that in LED-B compositional GQBs ($Al_xIn_yGa_zN$) are used instead of $Al_{0.55}Ga_{0.45}N$ QBs. The grading in the $Al_xIn_yGa_zN$ composition in the first GQB is x: 0.6 to 0.7, y: 0.03 to 0.05, and z: 0.37 to 0.25 while for remaining GQBs the composition is x: 0.7 to 0.8, y: 0.03 to 0.05, and z: 0.27 to 0.15. The reason behind the low indium content in the first GQB is to enhance the injection efficiency. The schematics of both LED-A and LED-B devices is shown in Fig. 1. Other necessary parameters used in this work include electron mobility of 100 cm^2/V·s, hole mobility of 10 cm^2/V·s, SRH of 10 ns, Auger coefficient of 1×10^{-30} cm^6/s and threading dislocation density of 1×10^9/cm^2. The size of both LEDs is of 300×300 μm^2 (Table 1).

3. Results and discussion

In Fig. 2, the computed energy band diagrams show that the QWs in LED-B are deeper than in LED-A. This indicates that LED-B QWs have better confinement of carriers compared to shallow LED-A QWs. In addition, the band tilt at the last quantum barrier/EBL interface is reversed in LED-B as compared to LED-A shown by a dotted circle in Fig. 2. The effective barrier height for holes in LED-B is reduced which is desired for the enhancement of hole concentration in the device active region. In LED-A

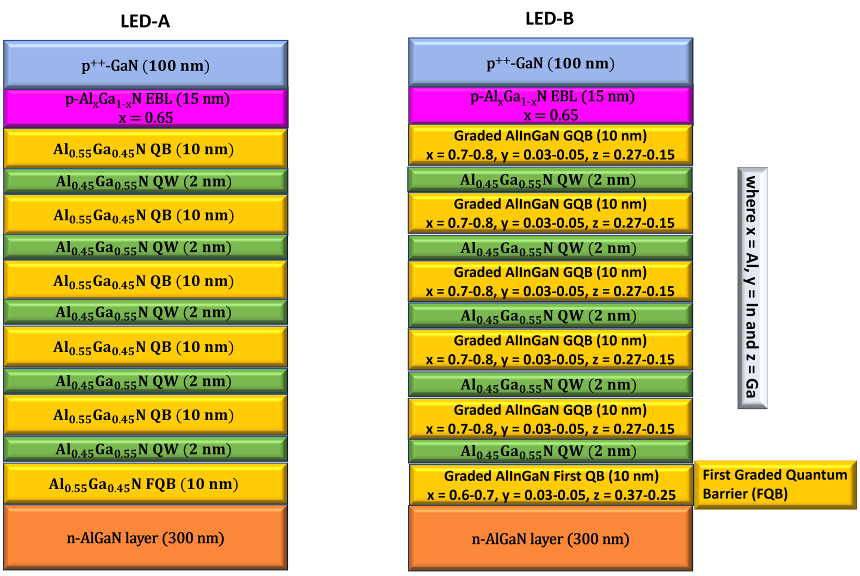

Fig. 1. Schematics of LED-A and LED-B.

Table 1. Structure parameters of LED-A and LED-B.

Device structure	SRH (ns)	Auger (cm^6/s)	Doping (cm^{-3})			Mobility (cm^2/V·s)		Al composition in Final Quantum Barrier		Thickness (nm)	
			n	p	p^{++}	Hole	Electron	LED-A	LED-B	LED-A	LED-B
n-$Al_{0.55}Ga_{0.45}N$	10	1×10^{-30}	5×10^{18}	NIL	NIL	10	100	0.55	0.45	300	300
$Al_xIn_yGa_zN$ First QB	10	1×10^{-30}	NIL	NIL	NIL	10	100	0.55	x = 0.6–0.7, y = 0.03–0.05, z = 0.37–0.25 (Graded)	10	10
$Al_{0.45}Ga_{0.55}N$ QWs	10	1×10^{-30}	NIL	NIL	NIL	10	100	0.45	0.55	2	2
$Al_xIn_yGa_zN$ QBs	10	1×10^{-30}	NIL	NIL	NIL	10	100	0.55	x = 0.7–0.8, y = 0.03–0.05, z = 0.37–0.15 (Graded)	10	10
$Al_{0.65}Ga_{0.35}N$ EBL	10	1×10^{-30}	NIL	5×10^{19}	NIL	10	100	0.65	0.35	15	15
p-GaN	10	1×10^{-30}	NIL	NIL	1×10^{20}	10	100	0	0	100	100

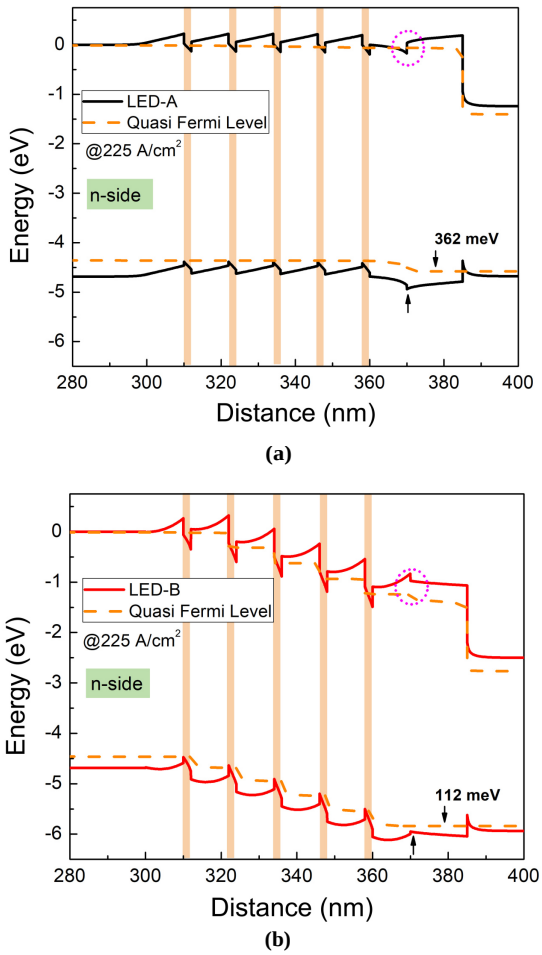

Fig. 2. Energy band diagrams of LED-A (a) and LED-B (b) compared at 225 A/cm^2.

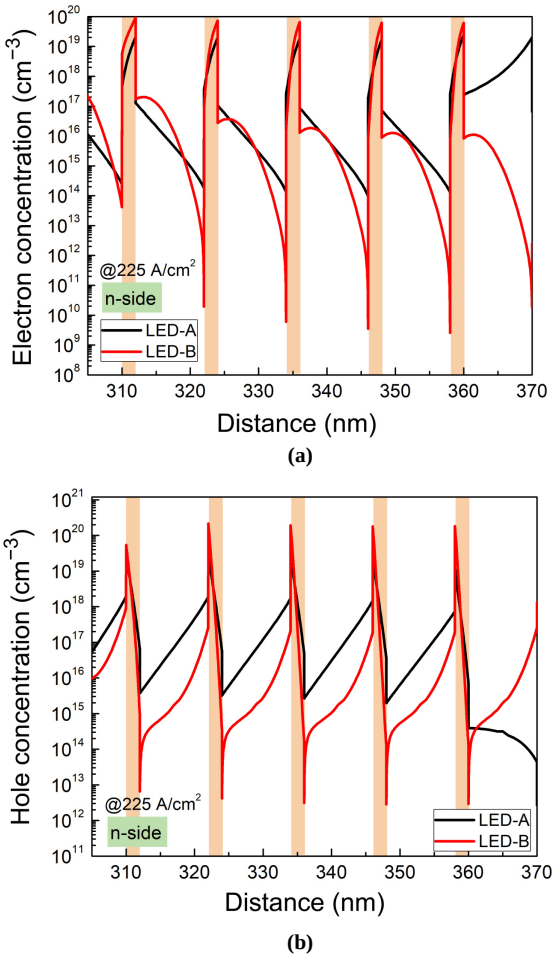

Fig. 3. Carrier concentrations of electrons (a) and holes (b) compared at 225 A/cm^2.

and LED-B, the effective barrier height for holes is of ~362 meV and 112 meV, respectively. It is pertinent to mention that in the multiquantum wells (MQWs) of the proposed structure, the electron concentration is enhanced in comparison to the conventional structure as shown in Fig. 3. The concentration of electrons in LED-B is increased by ~156% compared to LED-A. This enhancement is attributed to an increased barrier height for electrons because of using GQB. From Fig. 3(a), it can be observed that the increase in concentration of electrons in the first QW is higher compared to other QWs. This is due to the presence of a low Al composition in the first GQB compared to other GQBs which enhances the electron injection efficiency and, therefore, the concentration of electrons is higher in the first QW.

Likewise, the hole concentration is also increased in LED-B because of the reduction in the effective barrier height for holes which increases the transport and injection of holes inside the active region as shown in Fig. 3(b). The increase in the hole concentration in LED-B is of ~44% compared to LED-A. These results indicate that, by using GQBs, the overflow of electrons is mitigated and the hole injection is increased.

As a result of the increase carrier confinement in LED-B, the overlapping probability of carriers is also increased which results in an increased radiative recombination rate. Figure 4 shows the radiative recombination rate of two compared LEDs. In the proposed LED with

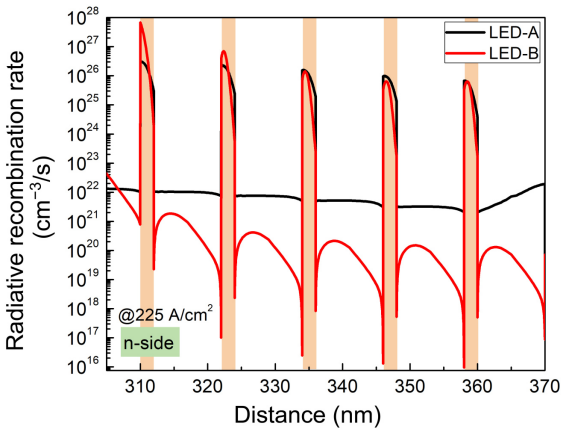

Fig. 4. Radiative recombination of LED-A and LED-B at 225 A/cm^2.

GQBs (LED-B), the increase in the radiative recombination rate is more than 400% with reference to LED-A.

The carrier flux with respect to the distance of the device in Fig. 5 has also been computed and analysed. From Fig. 5(a), it can be observed that the electrons flux towards the p-side is almost zero in case of our proposed structure (LED-B) as compared to the conventional LED-A. Meanwhile, the hole flux rises from the p-side towards the active region in LED-B as compared to LED-A as shown in Fig. 5(b). This is due to a decrease of the effective barrier height for holes.

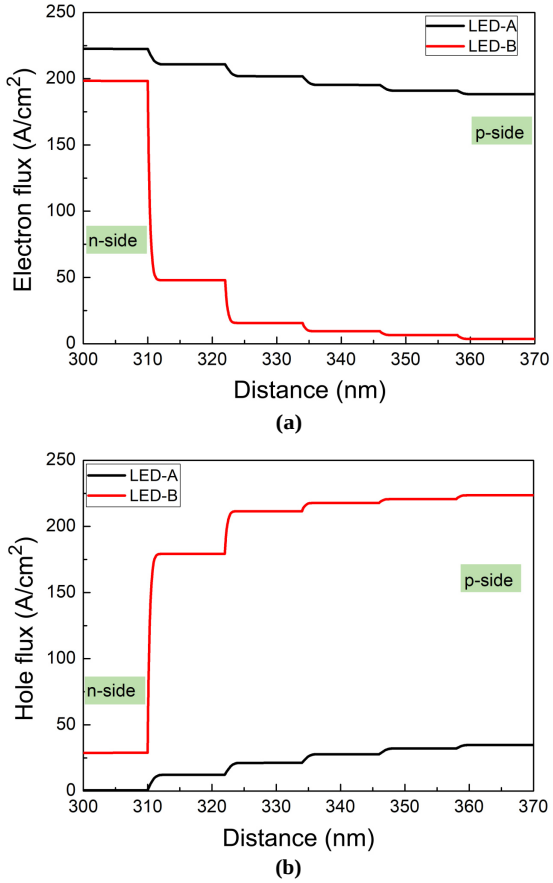

Fig. 5. Electron flux (a) and hole flux (b) comparison of two LEDs at 225 A/cm^2.

The efficiency droop in LED-A is remarkably high because of the conventional AlGaN quantum barriers shown in Fig. 6. However, the efficiency droop is significantly reduced in LED-B because of the use of GQBs. The efficiency droop in LED-A and LED-B is of ~77% and ~36%, respectively. Therefore, in our LED-B, not only an increased peak efficiency, but also a decreased efficiency is proposed.

In Fig. 7(a), the peak emission wavelength of both LEDs is nearly of 275 nm. The emission rate of LED-B is about three times higher than LED-A for the same current injection. This enhancement in LED-B is attributed to the improved internal quantum efficiency which resulted from the enhanced radiative recombination of carriers. The emission spectrum value is of critical importance in the UV range due to its wide range of applications. It is also interesting to note that high Al in multiquantum wells gives a shorter wavelength while low Al content gives a longer wavelength as shown in Fig. 7(b).

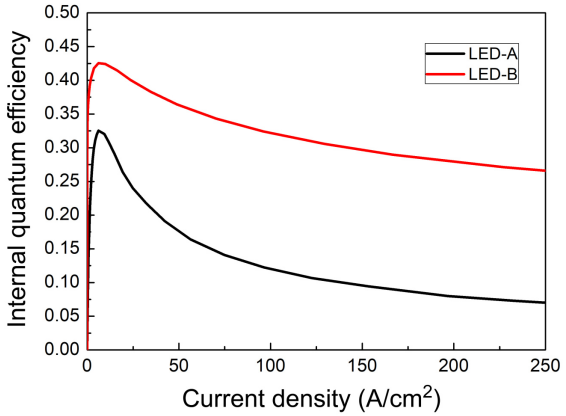

Fig. 6. Internal quantum efficiency of two LEDs being compared with respect to current density.

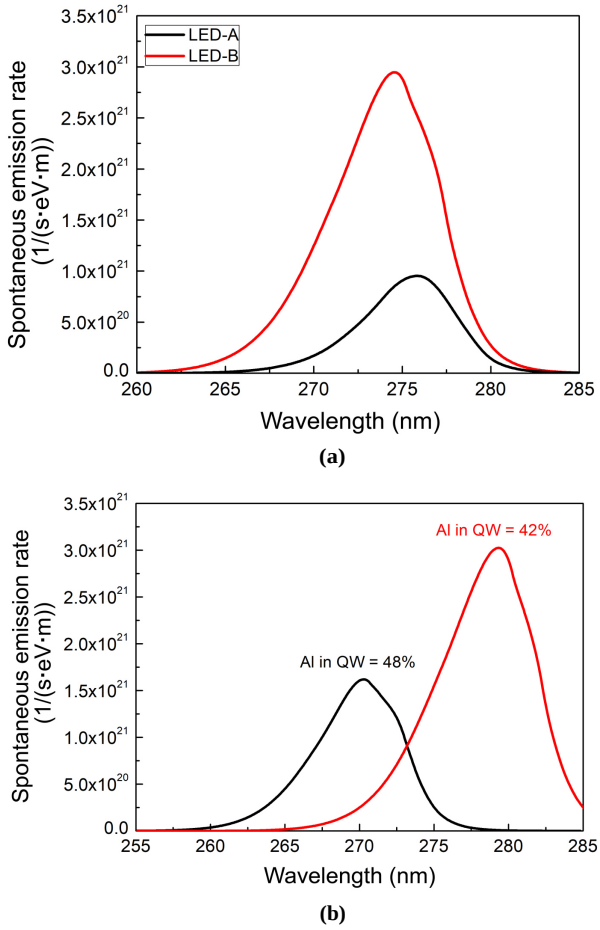

Fig. 7. Comparison of spontaneous emission of two LEDs (a), influence of aluminium quantum in the QW on emission spectrum at 225 A/cm^2 (b).

4. Conclusions

The optoelectronic characteristics of two LEDs, i.e., proposed LED (LED-B) and conventional LED (LED-A) were investigated. In LED-B, the conventional QBs were replaced by the compositional graded quaternary barriers (GQBs). Our results showed that the proposed device. with a better concentration of carriers in multiquantum wells has improved optoelectronic properties compared to the conventional structure. In our device structure of LED-B, the concentration of electrons and holes is increased by ~156% and ~44%, respectively compared to LED-A. Likewise, the radiative recombination rate in LED-B is increased more than ~400% compared to LED-A. The efficiency droop in LED-B equals ~36% compared to a ~77% droop of LED-A. It was concluded from all discussion that the proposed device is an efficient design for the future UV LEDs. Since UV radiation is widely used in sterilization and purification processes, as well as in suppression of viruses such as coronavirus (SARS-CoV-2) severe acute respiratory syndrome, our study can be helpful in attaining efficient UV light-emitting diodes.

Author statement

Research concept and design, S. M. and M. U., collection and/or assembly of data S. M., M. M., M. H., data analysis and interpretation, S. M., M. M., and M. U., writing of the article, S. M., M. M., M. U., critical revision of the article, S. M. and M. U., final approval of the article, S. M. and M. U.

Acknowledgements

The authors are grateful to the STR Group, Russia and the GIK Institute, Pakistan for providing technical support for this work.

References

[1] Würtele, M. *et al.* Application of GaN-based ultraviolet-C light emitting diodes–UV LEDs–for water disinfection. *Water Res.* **45,** 1481–1489 (2011), https://doi.org/10.1016/j.watres.2010.11.015

[2] Khan, A., Balakrishnan, K. & Katona, T. Ultraviolet light-emitting diodes based on group three nitrides. *Nat. Photonics* **2**, 77–84 (2008), https://doi.org/10.1038/nphoton.2007.293

[3] Usman, M., Malik, S. & Munsif, M. AlGaN-based ultraviolet light-emitting diodes: Challenges and Opportunities. *Luminescence* **36**, 294–305 (2021), https://doi.org/10.1002/bio.3965

[4] Hirayama, H., Maeda, N., Fujikawa, S., Toyoda, S. & Kamata, N. Recent progress and future prospects of AlGaN-based high-efficiency deep-ultraviolet light-emitting diodes. *Jpn. J. Appl. Phys.* **53**, 100209 (2014), http://doi.org/10.7567/JJAP.53.100209

[5] Kneissl, M. A brief review of III-nitride UV emitter technologies and their applications. in *III-Nitride Ultraviolet Emitters: Technology and Applications. Springer Series in Materials Science, vol 227*. (eds. Kneissl, M. & Rass, J.) 1–25 (Springer Cham, 2016). https://doi.org/10.1007/978-3-319-24100-5_1

[6] Usman, M., Malik, S., Khan, M. A. & Hirayama, H. Suppressing the efficiency droop in AlGaN-based UVB LEDs. *Nanotechnology* **32**, 215703 (2021), https://doi.org/10.1088/1361-6528/abe4f9

[7] Heilingloh, C. S. *et al.* Susceptibility of SARS-CoV-2 to UV irradiation. *Am. J. Infect. Control* **48**, 12731275 (2020), https://doi.org/10.1016/j.ajic.2020.07.031

[8] Khan, M. A., Shatalov, M., Maruska, H., Wang, H. & Kuokstis, E. III–nitride UV devices. *Jpn. J. Appl. Phys.* **44**, 7191 (2005), https://doi.org/10.1143/jjap.44.7191

[9] Kneissl, M. *et al*. Advances in group III-nitride-based deep UV light-emitting diode technology. *Semicond. Sci. Technol*. **26**, 014036 (2010), https://doi.org/10.1088/0268-1242/26/1/014036

[10] Shatalov, M. *et al.* AlGaN deep-ultraviolet light-emitting diodes with external quantum efficiency above 10%. *Appl. Phys. Express* **5**, 082101 (2012), https://doi.org/10.1143/apex.5.082101

[11] Pernot, C. *et al.* Development of high efficiency 255–355 nm AlGaN-based light-emitting diodes. *Phys. Status Solidi A* **208**, 1594–1596 (2011), https://doi.org/10.1002/pssa.201001037

[12] Huang, C., Zhang, H. & Sun, H. Ultraviolet optoelectronic devices based on AlGaN-SiC platform: Towards monolithic photonics integration system. *Nano Energy*, **77,** 105149 (2020), https://doi.org/10.1016/j.nanoen.2020.105149

[13] Chen, K. *et al.* Effect of dislocations on electrical and optical properties of n-type Al 0.34 Ga 0.66 N. *Appl. Phys. Lett.* **93**, 192108 (2008), https://doi.org/10.1063/1.3021076

[14] Hirayama, H., Tsukada, Y., Maeda, T. & Kamata, N. Marked enhancement in the efficiency of deep-ultraviolet AlGaN light-emitting diodes by using a multiquantum-barrier electron blocking layer. *Appl. Phys. Express* **3**, 031002 (2010), https://doi.org/10.1143/apex.3.031002

[15] Huang, M.-F. & Lu, T.-H. Optimization of the active-layer structure for the deep-UV AlGaN light-emitting diodes. *IEEE J. Quantum Electron.* **42**, 820–826 (2006), https://doi.org/10.1109/JQE.2006.877217

[16] Lu, L. *et al.* Improving performance of algan-based deep-ultraviolet light-emitting diodes by inserting a higher Al-content algan layer within the multiple quantum wells. *Phys. Status Solidi A* **214**, 1700461 (2017), https://doi.org/10.1002/pssa.201700461

[17] Arif, R. A., Ee, Y. K. & Tansu, N. Nanostructure engineering of staggered InGaN quantum wells light emitting diodes emitting at 420–510 nm. *Phys. Status Solidi A* **205**, 96–100 (2008), https://doi.org/10.1002/pssa.200777478

[18] Usman, M. *et al*. Zigzag-shaped quantum well engineering of green light-emitting diode. *Superlattices Microstruct.* **132**, 106164, (2019) https://doi.org/10.1016/j.spmi.2019.106164

[19] Usman, M. *et al.* Enhanced internal quantum efficiency of bandgap-engineered green W-shaped quantum well light-emitting diode. *Appl. Sci.* **9**, 77 (2019), https://doi.org/10.3390/app9010077

[20] Yang, G. *et al.* Design of deep ultraviolet light-emitting diodes with staggered AlGaN quantum wells. *Physica E* **62**, 55–58 (2014), https://doi.org/10.1016/j.physe.2014.04.014

[21] Zhang, Y. *et al.* The improvement of deep-ultraviolet light-emitting diodes with gradually decreasing Al content in AlGaN electron blocking layers. *Superlattices Microstruct.* **82**, 151–157 (2015), https://doi.org/10.1016/j.spmi.2015.02.004

[22] Li, Y. *et al.* Advantages of AlGaN-based 310-nm UV light-emitting diodes with Al content graded AlGaN electron blocking layers. *IEEE Photonics J.* **5**, 8200309–8200309 (2013), https://doi.org/10.1109/JPHOT.2013.2271718

[23] Fan, X. *et al.* Efficiency improvements in AlGaN-based deep ultraviolet light-emitting diodes using inverted-V-shaped graded Al composition electron blocking layer. *Superlattices Microstruct.* **88**, 467–473 (2015), https://doi.org/10.1016/j.spmi.2015.10.003

[24] Huang, J. *et al.* Study of deep ultraviolet light-emitting diodes with ap-AlInN/AlGaN superlattice electron-blocking layer. *J. Electron. Mater.* **46**, 4527–4531 (2017), https://doi.org/10.1007/s11664-017-5413-0

[25] Usman, M., Jamil, T., Malik, S. & Jamal, H. Designing anti-trapezoidal electron blocking layer for the amelioration of AlGaN-based deep ultraviolet light-emitting diodes internal quantum efficiency. *Optik* **232**, 166528 (2021). https://doi.org/10.1016/j.ijleo.2021.166528

[26] Zhang, X. *et al.* Efficiency improvements in AlGaN-based deep-ultraviolet light-emitting diodes with graded superlattice last quantum barrier and without electron blocking layer. *J. Electron. Mater.* **48**, 460–466 (2019). https://doi.org/10.1007/s11664-018-6716-5

[27] Li, K., Zeng, N., Liao, F. & Yin, Y. Investigations on deep ultraviolet light-emitting diodes with quaternary AlInGaN streamlined quantum barriers for reducing polarization effect. *Superlattices Microstruct.* **145**, 106601 (2020). https://doi.org/10.1016/j.spmi.2020.106601

[28] Shatalov, M. *et al.* Deep ultraviolet light-emitting diodes using quaternary AlInGaN multiple quantum wells. *IEEE J. Sel. Top. Quantum Electron.* **8**, 302–309 (2002). https://doi.org/10.1109/2944.999185

[29] Chen, X., Wang, D. & Fan, G. Investigation of AlGaN-based deep-ultraviolet light-emitting diodes with AlInGaN/AlInGaN super-lattice electron blocking layer. *J. Electron. Mater.* **48**, 2572–2576 (2019). https://doi.org/10.1007/s11664-019-07001-3

[30] Kim, S. J. & Kim, T. G. Numerical study of enhanced performance in InGaN light-emitting diodes with graded-composition AlGaInN barriers. *J. Opt. Soc. Korea* **17**, 16-21 (2013) . https://doi.org/10.3807/JOSK.2013.17.1.016

[31] Adivarahan, V. *et al.* Ultraviolet light-emitting diodes at 340 nm using quaternary AlInGaN multiple quantum wells. *Appl. Phys. Lett.* **79**, 4240–4242 (2001). https://doi.org/10.1063/1.1425453

[32] Chen, C. *et al.* Pulsed metalorganic chemical vapor deposition of quaternary AlInGaN layers and multiple quantum wells for ultraviolet light emission. *Jpn. J. Appl. Phys.* **41**, 1924 (2002). https://doi.org/10.1143/jjap.41.1924